Odorant receptors at the growth cone are coupled to localized cAMP and Ca^{2+} increases

Micol Maritan[a], Giovanni Monaco[a], Ilaria Zamparo[a], Manuela Zaccolo[b], Tullio Pozzan[a,c,d,1], and Claudia Lodovichi[a,1]

[a]Venetian Institute of Molecular Medicine, Via Orus 2, 35129 Padova, Italy; [b]Division of Biochemistry and Molecular Biology, Biomedical and Life Sciences, University of Glasgow, Glasgow G12 8QQ, United Kingdom; [c]Department of Biomedical Sciences, University of Padova, Viale G. Colombo 3, 35121 Padova, Italy; and [d]Consiglio Nazionale della Recherche, Institute of Neuroscience, 35121 Padova, Italy

Contributed by Tullio Pozzan, December 30, 2008 (sent for review December 1, 2008)

A distinctive feature in the topographic organization of the olfactory system in mammals is the dual function of the odorant receptor (OR): it detects odors in the nasal epithelium and plays an instructive role in the axonal convergence of olfactory sensory neurons (OSN) into the olfactory bulb (OB). The latter function is supported by genetic experiments and by the expression of the OR not only on the cilia, but also on the axon termini of the OSN. The signaling pathway coupled to the OR on the cilia is well known and is recognized to involve cAMP and Ca^{2+}, whereas, until now, nothing was known on the functional characteristics of the OR on the axon termini-growth cone. Here, by analyzing the spatiotemporal dynamics of cAMP and Ca^{2+} in living OSN *in vitro* and *in situ*, we found that the OR at the growth cone is capable of binding odors and is coupled to cAMP synthesis and Ca^{2+} influx through cyclic nucleotide gated (CNG) channels. Furthermore we found that selective odor activation of the OR on the growth cone is followed by nuclear translocation of protein kinase A catalytic subunit. These results define the functional properties of the OR on the growth cone and suggest a potential role of OR activation in axonal convergence and sensory map formation.

olfactory sensory neurons | real-time imaging | second messengers

In sensory systems, neurons in the peripheral sheet send their axons in precise loci of the CNS to create an internal representation of the external world. The spatial segregation of afferent inputs from primary sensory neurons provides a topographic map that defines the quality and the location of the stimulus. In the olfactory system, each OSN expresses only one OR gene out of a repertoire of approximately 1000 (1). OSNs expressing different ORs are randomly dispersed in the nasal epithelium. However, spatial order is achieved in the olfactory bulb (OB), where OSNs expressing the same odorant receptor converge with exquisite precision to form glomeruli both on the lateral and the medial side of each OB. Each odor is thus encoded by a specific spatial pattern of activated glomeruli. The OR, a G-protein-coupled receptor, upon binding of odorant ligands at the cilia, activates a specific G protein, Golf, that stimulates adenylyl cyclase, AC, to synthesize cAMP. The cAMP then directly activates cyclic nucleotide gated (CNG) channels, leading to action potential generation (2, 3).

A unique feature in the topographic organization of the OB is the "dual role" of the OR. Although it is well established that the OR is involved in the transduction of chemical signals (odors) at the cilia level, a number of evidence suggests that this receptor plays also an instructive role in glomerular convergence of OSN axons to the bulb (4–6). The latter property is supported by genetic observations demonstrating that alterations of OR sequence perturb the sensory map (7–9) and by the demonstration that the OR is expressed not only at the cilia but also on the OSN axon termini (10, 11). The OR is not the only determinant in proper glomeruli targeting, as OSNs expressing different receptors co-express different axon guidance molecules (12–14); but the link between these two phenomena remains largely mysterious.

However, until now, the key questions, i.e., whether the OR on the axon termini-growth cone is a functional receptor and which signaling pathway is coupled to it, remain unanswered. We addressed this question by analyzing the spatiotemporal dynamics of cAMP and Ca^{2+} in living OSNs in culture and *in situ*. Our data show that the OR at the growth cone is a functional receptor coupled to AC activation and to CNG channel-dependent Ca^{2+} influx. Selective activation of the OR at the growth cone resulted in nuclear translocation of the catalytic subunit of protein kinase A (PKA). Thus cAMP produced upon activation of the OR on the growth cone could have a major role in axonal convergence, acting locally and linking the OR identity with the expression of specific axon guidance molecules via PKA gene expression regulation.

Results

Spatial Patterns of cAMP Signaling in Cultured Olfactory Sensory Neurons. Primary cultures of OSN (identified by the expression of specific markers, [supporting information (SI) Fig. S1] were transiently transfected with the genetically encoded, PKA-based, fluorescent sensor for cAMP (15). Changes in $[cAMP]_i$ result in modification of fluorescence resonance energy transfer (FRET), between the YFP and CFP moieties genetically fused to the catalytic and regulatory subunit of PKA in the sensors, resulting in a change of the CFP/YFP fluorescence emission ratio. Fig. 1*A* shows the typical kinetic and spatial pattern of CFP/YFP fluorescence emission ratio (480 nm/545 nm) of a transfected OSN treated with forskolin, a generic activator of AC. Forskolin (3 μM) caused an increase in the 480/545 ratio, as expected for a rise in cAMP, in the cilia-dendrite, cell body, and axon termini-growth cone. The time for half maximal response ($t_{1/2}$) at the cilia-dendrite and axon termini-growth cone, however, is shorter than at the soma level ($n = 13$; $t_{1/2}$ in seconds: dendrite 46.8 ± 13.0, soma 92.2 ± 14.5, cone 41.7 ± 5.8; *t* test: dendrite-soma $P = 0.004$**, cone-soma $P = 0.002$**, dendrite-cone $P = 0.15$) (Fig. 1*B*). Application of isobutylmethyl-xanthine (IBMX), a nonselective inhibitor of phosphodiesterases (PDE), after this dose of forskolin, did not induce any further ratio increase (Fig. 1*A*). When OSNs were treated first with IBMX (100 μM), the rise in cAMP concentration was detected in all compartments and again faster at the cilia-dendrite and axon termini-growth cone than in the cell body ($n = 10$; $t_{1/2}$, in seconds: dendrite 174.4 ± 46.3, soma 228.8 ± 38.5, cone 133.6 ± 35.7; *t* test: dendrite-soma $P = 0.04$*, cone-soma $P = 0.007$**, cone-dendrite $P = 0.17$) (Fig. 1 *C* and *D*). In one third of the cells stimulated with IBMX, the subsequent challenge with forskolin induced a further rise in signal (Fig. 1*C*). Finally, upon simultaneous administration of forskolin and IBMX, the rise of cAMP remained faster at cilia-dendrite and at the axon termini-growth cone than at the soma

Author contributions: C.L. designed research; M.M. and G.M. performed research; I.Z. and M.Z. contributed new reagents/analytic tools; M.M. and G.M. analyzed data; and T.P. and C.L. wrote the paper.

The authors declare no conflict of interest.

Freely available online through the PNAS open access option.

[1]To whom correspondence may be addressed. E-mail: claudia.lodovichi@unipd.it or tullio.pozzan@unipd.it.

This article contains supporting information online at www.pnas.org/cgi/content/full/0813224106/DCSupplemental.

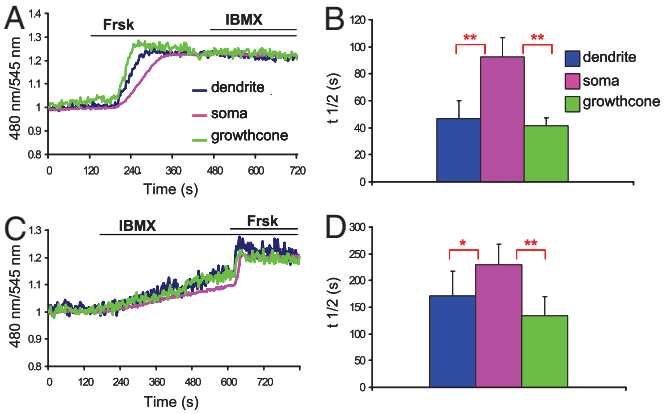

Fig. 1. cAMP dynamics in OSN. Normalized kinetics of fluorescence emission intensities (480 nm/545 nm) recorded in cilia-dendrite, soma, and axon termini-growth cone in OSN transfected with the PKA-based sensor and challenged with the following: (*A*) forskolin (Frsk,3 μM) and subsequently with IBMX (100 μM); (*C*) IBMX (100 μM) and subsequently with forskolin (25 μM); (*B*) and (*D*) time for half-maximal response ($t_{1/2}$) for cells treated with forskolin, (*B*) (dendrite-soma $P = 0.004$**, cone-soma $P = 0.002$**) and (*D*) IBMX (dendrite-soma $P = 0.04$*, cone-soma $P = 0.007$**); bars, SEM. The regions of interest (ROIs) were drawn on the distal part of the axon and dendrite and on the soma. The cilia were included in the dendrite ROI but were too thin to be clearly identified at the magnification used. Green line, axon termini-growth cone; pink line, soma; blue line, cilia-dendrite.

level ($n = 10$; $t_{1/2}$, in seconds: dendrite 56.1 ± 6.4; soma 87.0 ± 14.5; cone 51.3 ± 11.4; *t* test: dendrite-soma $P = 0.02$*, soma-cone $P = 0.001$**, dendrite-cone $P = 0.6$). Taken together the data indicate that: (*i*) the cAMP increases at the growth cone is due to local production of the second messenger and cannot be due to diffusion from cilia-dendrite or from the soma; and (*ii*) the AC has a sustained constitutive activity in OSN, and the basal concentration of cAMP is maintained low through the activity of PDEs. Thus, the molecular machinery required to produce and hydrolyze cAMP is present not only at the cilia but also at the growth cone level.

We next investigated whether the OR on the growth cone is functionally coupled to cAMP production. When OSNs were challenged with a bath application of an odor mixture, a rise in cAMP was elicited throughout the OSN. The rise in cAMP was again faster in the cilia-dendrites and axon termini-growth cone than at the soma level ($n = 12$; $t_{1/2}$, in seconds, dendrite 201.5 ± 33.3, soma 337.05 ± 54.7, cone168.3 ± 29.7, *t* test: dendrite-soma $P = 0.02$*, cone-soma, $P = 0.006$**) (Fig. 2 *A* and *B*, Movie S1). The cAMP increase remained, for the entire duration of the experiment (≈15 minutes), significantly lower at the soma than in other compartments (in three cells we did not detect any cAMP increase at the soma). To exclude a potential Ca^{2+}-dependent activation of the AC at the growth cone, secondary to the rise in Ca^{2+} associated to the activation of the OR at the cilia level, we challenged the OSN with the odor mixture while bathed in Ca^{2+}-free Ringer's solution (no rise in Ca^{2+} was observed in the latter case; not shown). Also in these conditions the cAMP was detected first, and at comparable time, at the neurites and later at the cell body ($n = 10$; $t_{1/2}$, in seconds, dendrite 250.5 ± 43.9, soma 341.8 ± 39.7, cone 218.5 ± 57.2; *t* test, dendrite-soma $P = 0.004$**, cone-soma $P = 0.002$**) (Fig. 2 *C* and *D*). Finally, we focally applied odorants to the growth cone, using a micropipette. Under these conditions a rise in cAMP was detected exclusively at the growth cone ($n = 10$; $t_{1/2}$, in seconds, 67.5 ± 18.3) (Fig. 2*E*), and no appreciable changes in signal were observed in the other compartments. It should be stressed that, although the rises in cAMP caused by the pharmacological treatments were observed in practically all neurons tested, the response to the odor mixture was observed in a subpopulation of neurons

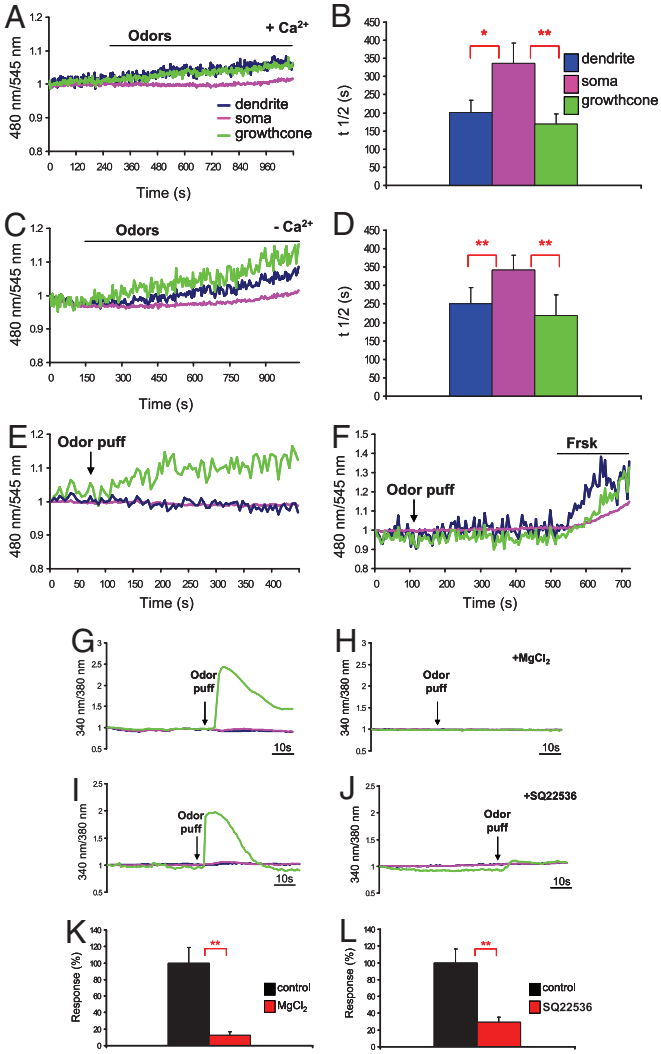

Fig. 2. cAMP and Ca^{2+} dynamics in OSN in response to odors. Conditions as in Fig. 1. (*A*) Odor mixture (200 μM) was applied to the bath in normal Ringer's solution. (*C*) As in (*A*) but in Ca^{2+} free Ringer's solution. (*E*) odor puff focally applied to the growth cone. (*B*) and (*D*) time for half-maximal response ($t_{1/2}$) for the related treatment, in (*B*) dendrite-soma $P = 0.02$*, cone-soma $P = 0.006$**; in (*D*) dendrite-soma $P = 0.004$**, cone-soma $P = 0.002$**; bars, SEM. (*F*) Example of OSN nonresponsive to the local odor puff but responsive to forskolin, bath applied. In (*G*) and (*I*), normalized fluorescence ratio changes (340 nm/380 nm) in two OSN loaded with Fura 2-AM and challenged with an odor puff focally applied to the growth cone. The same neurons of panel (*G*) and (*I*) were rechallenged with an odor puff in the presence of *H*, CNG channel blocker $MgCl_2$ (10 mM) or *J*, AC blocker, SQ22536 (30 μM). (*K* and *L*) Summary of responses (%), (*i*) $P = 0.002$**, (*L*) $P = 0.001$**, bars, SEM. Green line, axon termini-growth cone; pink line, soma; blue line, cilia-dendrite.

(30% of cells tested), as expected given the specificity of the OR expressed by each OSN.

Ca^{2+} Influx Through CNG Channels. The question then arises as to the possibility that the entire signal transduction machinery is functional at the growth cone-axon termini. It is well known that exposure of OSNs to odors stimulates at the cilia the influx of Ca^{2+} through CNG channels. To assess whether this signaling cascade takes place at the axon termini-growth cone as well, we measured the dynamics of Ca^{2+} upon odor stimulation of OSN loaded with the fluorescent Ca^{2+} indicator Fura-2. To avoid action potential contribution to the measured Ca^{2+} signal, all Ca^{2+} experiments were performed in presence of TTX. Fig. 2*G* shows the typical

kinetics of $[Ca^{2+}]$ changes elicited in a OSN by an odor mix puff applied to the growth cone with a micropipette: the odors induced a rapid and transient increase in $[Ca^{2+}]$ that remained confined to the axon termini-growth cone ($n = 15$, $\Delta R/Ro$ (%) = 102.6 ± 16.7). Notably, the $[Ca^{2+}]$ rise is much faster and more transient compared to the cAMP increase (see Discussion). Fig. 2*H* shows that when the same neuron in Fig. 2*G* was restimulated (15 minutes after washing away the stimulus) in the presence of the CNG channel blocker $MgCl_2$ (10 mM), no increase in $[Ca^{2+}]$ was observed (in 10 of 10 cells tested). Similarly, Fig. 2 *I* and *J* show that when the same odor-sensitive neuron (Fig. 2*I*) was restimulated in presence of the AC blocker SQ22536, the $[Ca^{2+}]$ rise was abolished (Fig. 2*J*) (in six of six cells tested). To exclude the possibility that the lack of response to odors in the presence of CNG channel or AC blockers was caused by desensitization of the OR after the first stimulation, the odor mix was applied first in the presence of the AC blocker and subsequently again on its own, 15 minutes after washing away the drug. No rise in $[Ca^{2+}]$ was ever detected in the presence of SQ22536, whereas, upon removal of the blocker, approximately 30% of the OSN (the normal % of responding neurons) underwent an increase in $[Ca^{2+}]$ upon odor mix application.

It has been suggested that the OR-derived cAMP signals regulate the transcription of genes encoding axon guidance molecules, which may in turn guide positioning of glomeruli (12–14, 16). To induce gene expression, the OR-derived cAMP signals need to somehow reach the nucleus, e.g., via translocation of the catalytic subunit of PKA. To test whether the cAMP rise triggered by the OR may be sufficient to induce such translocation, we followed the subcellular distribution of the YFP-tagged catalytic subunit of the transfected PKA-based sensor (PKA-C). As a control, we first treated the cells with forskolin (Fig. 3*A*). Whereas before stimulation the PKA-C was clearly excluded from the nucleus, 10 minutes after forskolin addition a fraction of PKA-C was clearly translocated in the OSN nucleus ($n = 4$). Fig. 3*B* shows that 10 minutes after an odor puff focally applied to the growth cone, the PKA-C is found also in the nucleus ($n = 8$).

Functional Properties and Signaling Pathway of the OR *ex Vivo*. The data presented above indicate that in OSN, in culture, the OR expressed at the growth cone is functional and coupled to cAMP synthesis and Ca^{2+} influx through CNG channels. The possibility, however, exists that this situation is a consequence of isolation and culture conditions and does not reflect the situation *in vivo*.

To assess whether the functional properties and the signaling pathway coupled to the OR in dissociated cells take place also in the intact OB, we performed Ca^{2+} imaging experiments on hemi-head explant preparations (17). In this preparation the mouse head is cut sagittally and the connections between the olfactory epithelium, the bulb and the brain are maintained along the medial axis. The Ca^{2+} indicator Calcium Green dextran was loaded in living mice (18) and resulted in strong labeling of OSN, from the cilia to the axon terminals in the glomeruli. A puff of forskolin, applied to the OB in the hemi-head preparation (incubated with 4 μM TTX), induced a clear rise in fluorescence (indicating a rise in $[Ca^{2+}]$) of labeled glomeruli (mice $n = 4$, glomeruli $n = 20$, $\Delta F/F_0 = 0.38 \pm 0.03$) (Fig. 4*A*). Under the same conditions, we applied odor puffs to labeled glomeruli in the OB. Upon odor stimulation, a rapid rise in $[Ca^{2+}]$ is observed in presynaptic terminals at the glomeruli level (mice $n = 9$, glomeruli $n = 23$, $\Delta F/F_0 = 0.44 \pm 0.06$) (Fig. 4*B*). The increase in $[Ca^{2+}]$ is due to cAMP-induced CNG channel opening, as this increase was abolished in the presence of the AC blocker SQ22536 (Fig. 5). Given the packing of glomeruli in the OB, an odor puff can reach several adjacent glomeruli. However, because of the molecular specificity of the OR in each glomerulus, approximately 30% of the stimulated glomeruli showed an increase in $[Ca^{2+}]$ (Fig. 4 and Movie S2). On the contrary, upon forskolin stimulation, all adjacent labeled glomeruli underwent a rise in $[Ca^{2+}]$.

Altogether, these data indicate that the ORs expressed at the axon termini of OSNs in a semi-intact preparation are capable of binding odors and are coupled to local cAMP synthesis and Ca^{2+} influx through CNG channels.

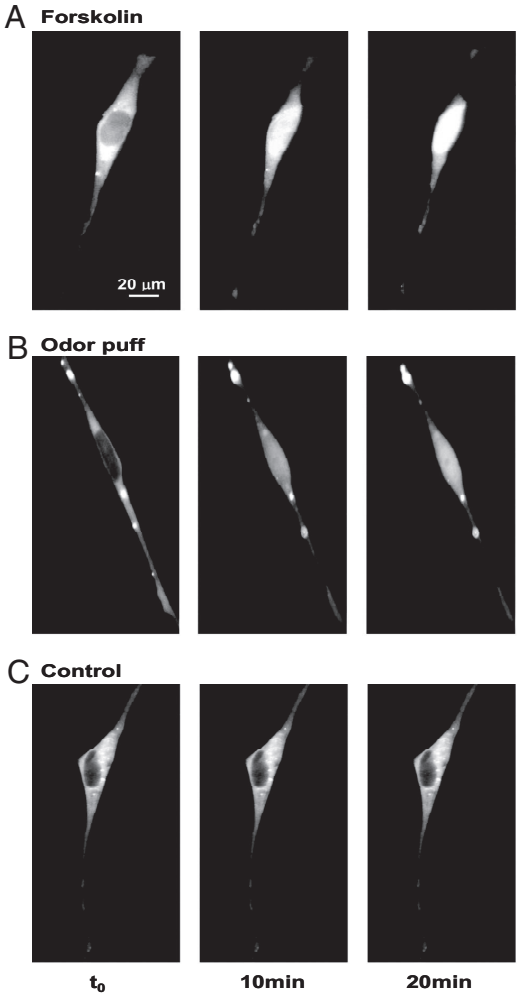

Fig. 3. C-PKA dynamics in OSN. Nuclear translocation of the YFP tagged catalytic subunit of the PKA sensor: basal condition (t_0), and 10 minutes and 20 minutes after (*A*) forskolin (25 μM) bath applied, and (*B*) after an odor puff, focally applied to the growth cone. (*C*) Control, illuminated as in *A* and *B* but without stimulation. The excitation and emission wavelengths were 500 and 545 nm, respectively. At these wavelengths, only YFP is excited and, accordingly, the fluorescence is insensitive to cAMP and only sensitive to the YFP concentration/distribution. In *B*, a few aggregates of PKA-C are found, as in approximately 40% of transfected OSNs.

Discussion

By analyzing the spatiotemporal dynamics of cAMP in OSN transfected with a genetically encoded fluorescent cAMP sensor based on PKA, we here demonstrate that both pharmacological agents (i.e., the AC stimulator forskolin and the PDE inhibitor IBMX) and physiological stimuli (odors) can induce cytosolic cAMP rise in the entire neuron, including the axon termini. We also show that, independently of the stimulus type, the speed of the cAMP increase in the OSN is faster in the neuronal processes (cilia-distal dendrite and axon termini-growth cone) than in the soma. At the moment, we cannot exclude the possibility that the rise in cAMP in the soma is caused by diffusion from the processes rather than to local production. Most important, however, the cAMP produced upon odor stimulation at the growth cone is due to activation of the OR in this location and

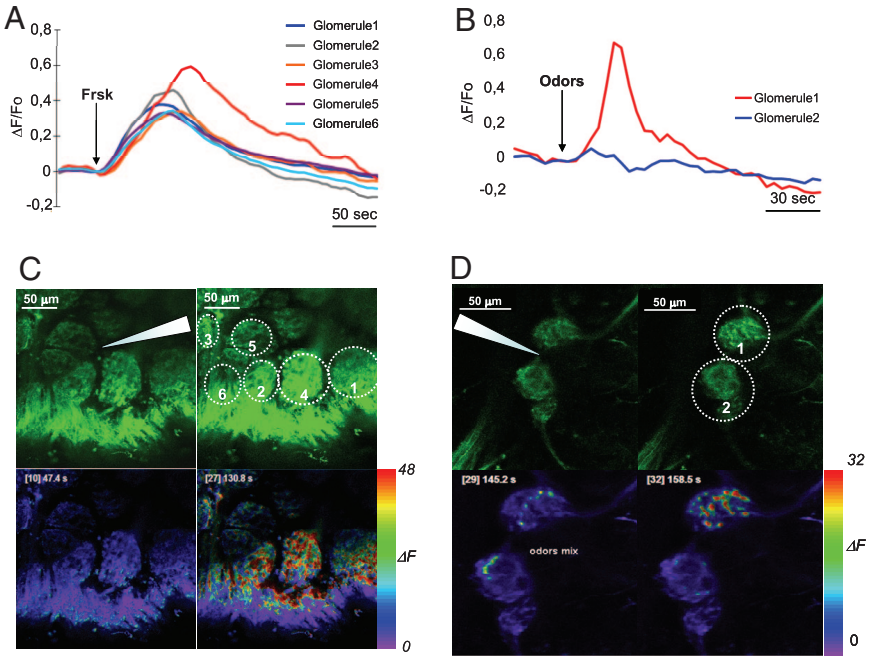

Fig. 4. [Ca^{2+}] dynamics in glomeruli. (*A* and *B*) Changes in fluorescence ($\Delta F/F_0$) in different glomeruli in hemi-head preparations after focal stimulation with (*A*) forskolin (Frsk, 250 μM in pipette) or (*B*) odor mixture (1 mM in pipette). (*C Upper* and *D Upper*) Images of Calcium Green dextran loaded glomeruli; before (*Left*) and after (*Right*) forskolin (*C Upper*) or odor stimulation (*D Upper*). (*C Lower* and *D Lower*) The images are presented in pseudocolors. Bar on *right* represents the pseudocolor scale of the difference in fluorescence intensity, ΔF (in arbitrary units), between the peak of the response (*Right*) and the basal condition (*Left*) of forskolin (*C Lower*) and odor mixture application (*D Lower*). Arrowheads indicate stimulus-pipette position; colored lines and circles indicate glomeruli.

not to indirect effects, e.g., cAMP diffusion from the other compartments or Ca^{2+}dependent activation of the AC.

These data are in agreement with the distribution of AC, as revealed by immunohistochemical localization. The protein level is highly enriched in OSN dendrite endings and in the axonal projection, including the olfactory nerve layer and the glomeruli, but it is barely detectable at the soma (19). We also found that the signaling cascade known to be activated by odors at the cilia can be set in action by the OR expressed on the axon termini-growth cone. Local application of odors to the growth cone in fact results in a local increase in the [Ca^{2+}] through CNG channels. A comparison between the kinetics of cAMP and [Ca^{2+}] increase, whether applied to the bath or locally to the growth cone, however, reveals that these two signals have a very different temporal pattern: (*i*) the rise in [Ca^{2+}] is rapid (with our time resolution, one image/s, no appreciable lag phase is observed between the addition of the odor mix and the onset of the [Ca^{2+}] increase) and transient (the peak is reached in 3–5 seconds and [Ca^{2+}] is back close to the prestimulatory level within 30–60 seconds); (*ii*) on the contrary, the rise in cAMP is slower in onset and sustained, i.e., it shows no tendency to decrease for at least 5–10 minutes after odor application. The simplest explanation for these different kinetic patterns is that the CNG channels are exquisitely sensitive to the local concentration of cAMP underneath the plasma membrane, generated by OR activation (20–22). An alternative explanation, i.e., a higher affinity for cAMP of the CNG channels with respect to the PKA, seems to be excluded, as the affinity for cAMP of the regulatory subunit of the PKA (and of our sensor) is higher than that of the CNG channels (23, 24). The transient nature of the Ca^{2+} signal, and the prolonged duration of the cAMP rise, imply that the CNG channels inactivate

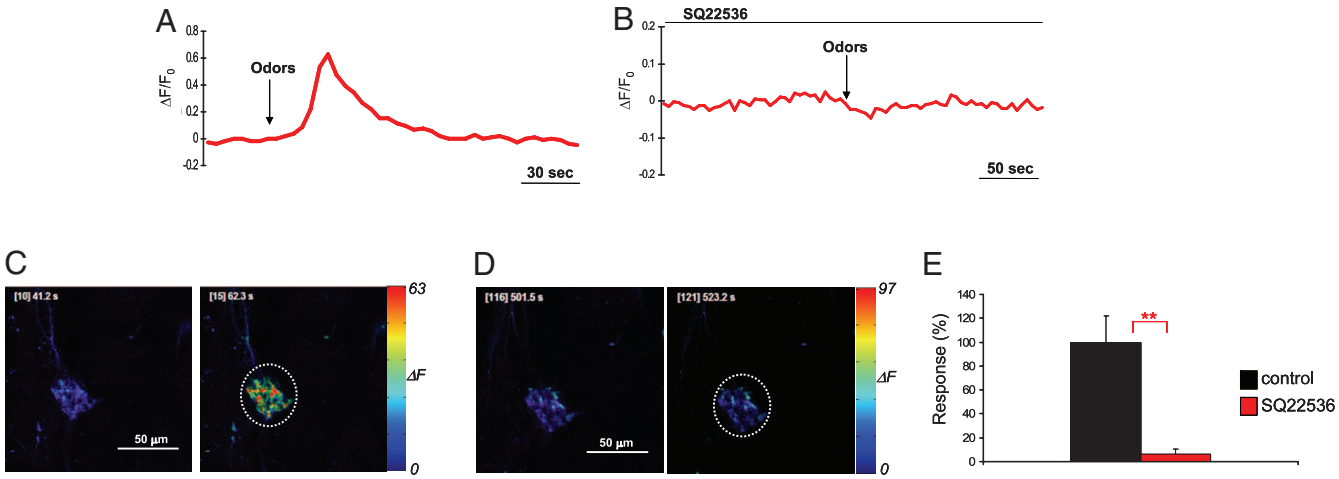

Fig. 5. [Ca^{2+}] dynamics in glomeruli: role of CNG channels. (*A*) Kinetic changes in fluorescence ($\Delta F/F_0$) in axon termini of OSN in hemi-head preparation challenged with an odor puff applied locally under control conditions. (*B*) Same glomerulus as in *A*, but challenged with an odor puff in the presence of the AC blocker, SQ22536. In *C* and *D* the pseudocolor images showing the images of the same glomerulus the fluorescence kinetic changes of which are shown in *A* and *B*. Images in *C* refer to the glomerulus in control conditions and those in *D* to the same glomerulus treated with the AC inhibitor. After the first stimulation the hemi-head was extensively washed with fresh medium and the second challenge with the odors in the presence of the AC inhibitor carried out 15 minutes after the first. (*E*) Summary of response (%) (mice, $n = 4$; glomeruli, $n = 4$; $P = 0.01$**; bars, SEM). ACSF was supplemented with TTX (4 μM) in all experiments. White circle indicates responding glomerulus.

more rapidly (or more extensively) than the OR, at least in the present experimental conditions.

Experiments carried out in the hemi-head preparation exclude the possibility that our findings in OSN in culture are influenced by the isolation procedure and culture conditions. By loading the OSN *in vivo* with a fluorescent Ca^{2+} indicator, we could demonstrate that the local application to the glomeruli of a pharmacological AC stimulator or, most important, odors results in a rapid and transient rise in $[Ca^{2+}]$ at the presynaptic terminals, with a kinetic pattern closely resembling that obtained in the cultured neurons. In addition, as expected for an OR coupled to AC activation, the Ca^{2+} increase by the odors was completely blocked by an AC inhibitor.

The question then arises as to the functional role of the cAMP and Ca^{2+} increases that can be generated by OR activation at the axon termini. An obvious candidate target is the axon path-finding process. This is a very complex phenomenon involving several steps. In the olfactory system, at least two events can be identified: the convergence of like axons to form glomeruli, and the location of the glomeruli in specific sites of the OB. It has been proposed that the OR derived cAMP signal plays a critical role in axonal convergence by modulating the expression of axon guidance molecules. In this model, the site of OR location and of cAMP production may appear irrelevant (13, 14). However, Golf knock out animals are anosmic but have a preserved map formation (25), thus excluding that cAMP formed at the cilia could play any major role in axonal convergence and glomeruli location. On the contrary, our finding that the OR at the axon termini is fully functional appears consistent with the hypothesis that axon termini OR act as guidance molecules through the local production of cAMP and Ca^{2+}. Indeed the role of cAMP and Ca^{2+} in axon guidance at the growth cone has been extensively studied in other system, and it has been shown that the local levels of these second messengers can modulate the behavior of the growth cone in response to external cues (26).

Preservation of axonal convergence and map formation in animals lacking Golf can be explained by the observation that Gs is expressed at the axon termini (and thus potentially coupled to local cAMP formation), not only in early stages of development (16, 25) but also in adulthood (Fig. S2). The presence of a functional OR on the axon termini-growth cone could also play a role in mediating contacts with postsynaptic cells. It is in fact known that: (*i*) the OR is essential not only for OSN axonal convergence but also for the formation of the intrabulbar link between homologous glomeruli (17, 27); and (*ii*) cyclic nucleotides acting at the axon termini can modulate synaptic transmission between the OSN and the postsynaptic cells (28, 29).

Finally, we also found that selective activation of the OR at the growth cone is followed by PKA C nuclear translocation. Thus the cAMP produced upon activation of the OR at the growth cone can act not only locally but also at the nuclear level modulating the expression of molecules involved in axon targeting. Although the local cAMP action is rapid and could determine the growth cone behavior in response to local cues, PKA-dependent gene expression is a long-term process that could intervene over a longer time period, e.g., to determine the position of the glomerulus in the bulb (12–14).

Other hypotheses have been proposed to explain the functional role of the OR expressed at the growth cone. For example it has been suggested that axonal convergence depends on homophilic OR interactions (9, 14). Although we have not addressed this possibility in the present work, the demonstration that the OR on the axon termini are functionally coupled to AC and CNG channel activation appears more in line with the idea that neurons expressing the same OR find their own path, responding to guidance cues that locally activate their OR.

As to the ligands able to activate the OR on the growth cone, we found that odors are able to activate the OR expressed on the growth cone in cultured neurons and, most important, *in situ*. It is tempting to speculate that the odorants themselves might be the ligand of the OR also at the growth cone. They are the only known specific ligands of the OR and the only molecules known to date that are capable of distinguishing among thousands of structurally identical but molecularly distinct receptors. Several mechanisms can be proposed on the pathway followed by odors to reach and activate the OR on the growth cone: vesicular transport, or diffusion along the membrane or through blood vessels. At the moment, we cannot exclude alternative mechanisms of activation of the OR at the axon terminal, such as OR constitutive activity or other OR activating molecules present in the bulb. Whatever the mechanism of activation of the OR on the growth cone, the finding that the OR on the axonal terminal is a functional receptor is the first essential step in dissecting the role of the OR on axon termini.

Materials and Methods

Primary Culture of Olfactory Sensory Neurons (OSN). The olfactory epithelium (OE) was harvested from embryonic rats (E 18) in ice-cold Hank's balanced salt solution (HBSS) (Invitrogen). Tissue was enzymatically dissociated and the resultant cell suspension was plated onto 24-mm glass coverslips coated with polyL lysine (Sigma) and maintained in culture medium (D-Val Mem, 10% fetal bovine serum [FBS], 5% Nu Serum, Penstrep L-glutamine, 100 U/ml (Invitrogen), 10 μM Ara C (Sigma), 25 ng/ml NGF (BD Biosciences) under standard conditions (30). After 24 hours in culture, the medium was changed and the cells were either transiently transfected with the PKA based sensor for cAMP with Transfectin (BioRad) transfection reagent or loaded with 5 μM Fura 2-AM (Molecular Probes) at 37 °C for 40 minutes. The PKA sensor used is a minor modification of the previously published probe (16) endowed with a slightly higher affinity for cAMP and an improved dynamic range in response to cAMP (I.Z. and M.Z., unpublished).

All cells used in this study were clearly identifiable as OSN by their characteristic bipolar morphology, having a single thick dendrite with knob-like swelling and cilia emanating from it, and a thin long axon. OSN in culture expressed the specific marker olfactory marker OMP (Fig. S1*A*). After transfection, cells were maintained in culture for additional 24 hours before FRET imaging experiments. In transfected cells, the fluorescence is evenly distributed throughout the cytoplasm and is excluded from the nucleus (Fig. S1*B*).

cAMP and Ca^{2+} Measurements in Cultured Neurons. cAMP and Ca^{2+} imaging experiments were performed on an inverted microscope (IX 81; Olympus) with a 60X NA 1.4 oil immersion objective (Olympus). The microscope was equipped with a CCD camera (SIS F-View), an illumination system MT20 (Olympus), and a beam-splitter optical device (Multispec Microimager; Optical Insights).

The day of the experiment, coverslips were mounted in a thermostated chamber at 37 °C (Warner Instruments) and maintained in Ringer's solution (in mM: 140 NaCl, 5 KCl, 1 $CaCl_2$ $2H_2O$, 1 $MgCl_2$, 10 HEPES, 10 glucose, 1 sodium pyruvate, pH 7.2) or Ca^{2+} free Ringer's solution (in mM: 140 NaCl, 5KCl, 1$MgCl_2$, 10 HEPES, 10 glucose, 1 sodium pyruvate, pH 7.2) supplemented with 1 mM EGTA. Images were acquired using Cell$^{\blacktriangle}$R software and processed off line using a custom-made software (V imaging made in Mat Lab environment). FRET changes were measured as changes in the background subtracted 480 nm/545 nm fluorescence emission intensities on excitation at 430 nm and expressed as R/R_0 where R is the ratio at time t and R_0 is the ratio at time = 0 seconds. The time for half-maximal response ($t_{1/2}$) was evaluated as the time, after stimulus application, at which half maximal response was reached, considering half maximal response = $(R-R_0)/2 + R_0$, and $t = t - t_0$, where t_0 is stimulus application time.

For the nuclear translocation of the YFP tagged catalytic subunit of PKA, we evaluated the changes in fluorescence (excitation filter 500 nm, emission filter 545 nm) at the nuclear level before and after stimulus application (bath or puff applied).

To avoid action potential contribution to the measured Ca^{2+} signal, 4 μM TTX (Latoxan) was added to the Ringer's solution in all Ca^{2+} imaging experiments. Changes in intracellular Ca^{2+} were visualized using 380-nm and 340-nm excitation filters and 510/40-nm emission filter and were acquired every second. Images were then processed off-line using ImageJ (National Institutes of Health, Bethesda, MD). Changes in fluorescence (340 nm/380 nm) was expressed as R/R_0, where R is the ratio at time t and R_0 is the ratio at time = 0 seconds. Response (%) were evaluated as $\Delta R/R_0 \times 100$ where $\Delta R = R - R_0$.

Stimuli on OSN *in Vitro*. Pharmacological stimuli, forskolin (3 μM and 25 μM), IBMX (100 μM), SQ22536 (30 μM), $MgCl_2$ (10 mM), all from Sigma, were prepared in stocks and diluted to the final concentration (indicated in brackets) in the bath. Forskolin 3 μM represented the lowest concentration at which we could obtained reproducible large FRET changes. The odorant stimuli were represented by mixtures of several compounds including: citralva, citronellal, menthone, carvone, eugenol, geraniol, acethophenone, hexanal, benzyl alcohol, heptanoic

acid, propionic acid, benzaldehyde, (all from Sigma) prepared as 1 mM stock in Ringer's solution and diluted to the final concentration of 200 μM in the bath. This stimulus concentration is well within the range (1 nM-1 mM) of those used in previous studies (31) on dissociated OSN, and it is the lowest concentration at which we could obtain reproducible responses.

Odor stimuli were also focally applied to the growth cone of OSN in culture by pressure injections (Pneumatic pico-pump, WPI) with a micropipette (3–5 μm tip diameter, 3-second puff duration). The micropipette was positioned at 5–10 μm from the growth cone. The preparation was continuously perfused with Ringer's solution (1.5 ml/min).Odor mixture concentration in the micropipette was 1 mM.

Ca^{2+} Imaging in Hemi-Head Preparation. Experiments were performed using postnatal day 8–22, (P8-P22) C57/B6 mice (Charles River). Olfactory sensory neurons were loaded *in vivo* with Calcium-Green-1 dextran, 10 KDa MW (Molecular Probes) following the protocol adapted from Wachowiack and Cohen (18). Three-four days after loading the dye, mice were deeply anesthetized with Zoletil 100 (a combination of Zolazapam and Tiletamine, 1:1, 10 mg/kg, Laboratoire Virbac) and Xilor (Xilazine 2%, 0.06 ml/kg, Bio98), decapitated, and the head cut sagittally (hemi-head explant preparations). The hemi-head was then placed in a custom-made imaging chamber, in ACSF (in mM.: 119 NaCl, 1,3 Mg SO_4, 2,5 $CaCl_2$ 2 H_2O, 2,5 KCl, 1 KH_2PO_4, 26,2 $NaHCO_3$, 11 glucose) and bubbled with 95% O_2 and 5% CO_2. A laser scanning confocal system (Bio-Rad Radiance 2100) attached to a Nikon Eclipse E 600-FN upright microscope was used to visualize changes in Calcium-Green fluorescence. The confocal system was equipped with Argon laser. A 40X NA 0.80 water immersion objective (Nikon, Fluor) was used. The excitation illumination was 514 nm and the emitted fluorescence was collected with a HQ 545/40 nm filter. Images were acquired with a resolution of 512 $\times$ 512 pixel under control of Bio Rad-LaserSharp 2000 software. All data were processed off line using a custom made software (V imaging made in Mat Lab environment).

Stimuli on Hemi-Head Preparation. To avoid action potential contribution to the measured Ca^{2+} signal, 4 μM TTX were added, at least 5 minutes before initiating the experiments, to the ACSF solution in all experiments. Stimuli were pressure injected (pneumatic pico-pump, WPI) with a micropipette (3–5-μm tip diameter) located above the glomeruli (distance $\approx$40 μm) in the olfactory bulb. Concentration of the stimuli in the pipette were: 250 μm forskolin, 1 mM odor mixture and 500 μM SQ22536. Puff duration was 60 seconds. The rise in $[Ca^{2+}]$ as induced by forskolin or odors initiates within 1–3 seconds from the odor puff application to the OB and thus excludes that this effect could be due to diffusion of the odor mix to the OSN cilia that are located at a distance of $\approx$1 cm.

Immunostaining. ***OMP.*** After 48 hours in culture, cells were fixed in ice-cold methanol 100% for 20 minutes at $-$20 °C. Cells were then reacted with goat polyclonal antibodies specific for OMP (Wako Chemicals) at 1:1000 dilution. The bound primary antibody was visualized using Cy3 conjugated anti-goat IgG (Jackson Laboratories).

Gs. Rats and mice P2-P20 were transcardially perfused with PBS, followed by 4% paraformaldehyde in PBS, ph 7.4. Brains were quickly removed and cryoprotected in 30% sucrose overnight. Coronal sections (20 μm) through the olfactory bulb were cut with a cryostat microtome. Tissue was then reacted with rabbit polyclonal antibodies specific for Gs (1:100, Millipore) and with goat polyclonal antibodies specific for OMP (1:20.000, Wako Chemicals). The bound primary antibodies were then visualized using a Cy3 conjugated anti-goat and Cy2 conjugated anti-rabbit (Jackson Laboratories).

All data are presented as mean $\pm$ standard error. Student's t tests (two-tailed, paired) were performed to evaluate statistical significance; *, $0.01 < P < 0.05$; **, $0.001 < P < 0.01$; ***, $P < 0.001$. The number of cells, animals, or glomeruli analyzed is denoted by ''n.''

ACKNOWLEDGMENTS. We thank Raffaella Flaibani for helping with experiments and all members of our laboratory for valuable comments. C.L. is an Armenise-Harvard Career Development Award recipient. This work was supported in part by grants from Human Frontier Science Program Organization (RGP0001/2005-C), the Fondation Leducq (O6 CVD 02), and the European Commission (LSHB-CT-2006-037189) (to M.Z.); and the Cariparo Foundation and Italian Ministery of the University (T.P.).

1. Buck L, Axel R (1991) A novel multigene family may encode odorant receptors: A molecular basis for odor recognition. *Cell* 65:175–187.
2. Menini A (1999) Calcium signalling and regulation in olfactory neurons. *Curr Opin Neurobiol* 9:419–426.
3. Malnic B, Hirono J, Sato T, Buck LB (1999) Combinatorial receptor codes for odors. *Cell* 96:713–723.
4. Reed RR (2003) The contribution of signaling pathways to olfactory organization and development. *Curr Opin Neurobiol* 13:482–486.
5. Ressler KJ, Sullivan SL, Buck LB (1994) Information coding in the olfactory system: Evidence for a stereotyped and highly organized epitope map in the olfactory bulb. *Cell* 79:1245–1255.
6. Vassar R, *et al*. (1994) Topographic organization of sensory projections to the olfactory bulb. *Cell* 79:981–991.
7. Mombaerts P, *et al.* (1996) Visualizing an olfactory sensory map. *Cell* 87:675–686.
8. Wang F, Nemes A, Mendelsohn M, Axel R (1998) Odorant receptors govern the formation of a precise topographic map. *Cell* 93:47–60.
9. Feinstein P, Bozza T, Rodriguez I, Vassalli A, Mombaerts P (2004) Axon guidance of mouse olfactory sensory neurons by odorant receptors and the beta2 adrenergic receptor. *Cell* 117:833–846.
10. Barnea G, *et al.* (2004) Odorant receptors on axon termini in the brain. *Science* 304:1468.
11. Strotmann J, Levai O, Fleischer J, Schwarzenbacher K, Breer H (2004) Olfactory receptor proteins in axonal processes of chemosensory neurons. *J Neurosci* 24:7754–7761.
12. Cutforth T, *et al.* (2003) Axonal ephrin-As and odorant receptors: Coordinate determination of the olfactory sensory map. *Cell* 114:311–322.
13. Imai T, Suzuki M, Sakano H (2006) Odorant receptor-derived cAMP signals direct axonal targeting. *Science* 314:657–661.
14. Serizawa S, *et al*. (2006) A neuronal identity code for the odorant receptor-specific and activity-dependent axon sorting. *Cell* 127:1057–1069.
15. Zaccolo M, Pozzan T (2002) Discrete microdomains with high concentration of cAMP in stimulated rat neonatal cardiac myocytes. *Science* 295:1711–1715.
16. Chesler AT, *et al.* (2007) A G protein/cAMP signal cascade is required for axonal convergence into olfactory glomeruli. *Proc Natl Acad Sci USA* 104:1039–1044.
17. Lodovichi C, Belluscio L, Katz LC (2003) Functional topography of connections linking mirror-symmetric maps in the mouse olfactory bulb. *Neuron* 38:265–276.
18. Wachowiak M, Cohen LB (2001) Representation of odorants by receptor neuron input to the mouse olfactory bulb. *Neuron* 32:723–735.
19. Col JA, Matsuo T, Storm DR, Rodriguez I (2007) Adenylyl cyclase-dependent axonal targeting in the olfactory system. *Development* 134:2481–2489.
20. Zaccolo M, *et al*. (2006) Restricted diffusion of a freely diffusible second messenger: Mechanisms underlying compartmentalized cAMP signalling. *Biochem Soc Trans* 34:495–497.
21. Davare MA, *et al.* (2001) A β_2 adrenergic receptor signaling complex assembled with the Ca^{2+} channel $Ca_V1.2$ *Science* 293:98–101.
22. Karpen JW, Rich TC (2005) High-resolution measurements of cyclic adenosine monophosphate signals in 3D microdomains. *Methods Mol Biol* 307:15–26.
23. Beavo JA, Bechtel PJ, Krebs EG (1974) Activation of protein kinase by physiological concentrations of cyclic AMP. *Proc Natl Acad Sci USA* 71:3580–3583.
24. Zagotta WN, Siegelbaum SA (1996) Structure and function of cyclic nucleotide-gated channels. *Annu Rev Neurosci* 19:235–263.
25. Belluscio L, Gold GH, Nemes A, Axel R (1998) Mice deficient in G(olf) are anosmic. *Neuron* 20:69–81.
26. Song HJ, Ming GL, Poo MM (1997) cAMP-induced switching in turning direction of nerve growth cones. *Nature* 388:275–279.
27. Belluscio L, Lodovichi C, Feinstein P, Mombaerts P, Katz LC (2002) Odorant receptors instruct functional circuitry in the mouse olfactory bulb. *Nature* 419:296–300.
28. Murphy GJ, Isaacson JS (2003) Presynaptic cyclic nucleotide-gated ion channels modulate neurotransmission in the mammalian olfactory bulb. *Neuron* 37:639–647.
29. Kafitz KW, Leinders-Zufall T, Zufall F, Greer CA (2000) Cyclic GMP evoked calcium transients in olfactory receptor cell growth cones. *Neuroreport* 11:677–681.
30. Ronnett GV, Hester LD, Snyder SH (1991) Primary culture of neonatal rat olfactory neurons. *J Neurosci* 11:1243–1255.
31. Bozza TC, Kauer JS (1998) Odorant response properties of convergent olfactory receptor neurons. *J Neurosci* 18:4560–4569.